

NR LATEX COATED NANO ZnO DISKS FOR POTENTIAL DIELECTRIC APPLICATIONS

D. THOMAS^{a, b*}, S. AUGUSTINE^b, J. PRAKASH^c

^aResearch and Development Centre, Bharathiar University, Coimbatore, India-641046

^bResearch and Post-Graduate Department of Physics, St.Thomas College, Pala, Kottayam, India-686574

^cResearch and Post-Graduate Department of Chemistry, St.Thomas College, Pala, Kottayam, India-686574

The present study focuses on the synthesis of ZnO nanoparticles of varying size (40-100nm) by reverse micelle method using sodium dodecyl sulphide as stabilising agent. The variation in size was obtained by changing the calcination temperature. The nanocrystalline nature of the prepared samples was investigated using different techniques such as UV-Visible spectrophotometer, IR spectrometer, XRD, SEM, TEM. The prepared powder samples were then pressed into disks and coated with natural rubber (NR latex) using dip coating technique. The dielectric studies of the nano ZnO- rubber disks were then carried out at varying frequencies. The effect of particle size on dielectric constant, dielectric loss, ac conductivity and Q factor was examined. It was found that all the parameters are very sensitive to the size of the particle. The parameters can be tuned to desired values by varying the particle size. The Particles calcinated at 550°C, having minimum size, show the most promising results.

(Received September 1, 2014; Accepted October 13, 2014)

Keywords: ZnO powder SDS Calcination Temperature Nano ZnO rubber disks

1. Introduction

The research on semiconductor nanostructures has great importance in recent years due to their optical, electrical and photocatalytic properties. The unique properties of semiconductor nanostructures are due to quantum effects and increased surface to volume ratio [1]. The different semiconducting nanomaterials of single elements, compound semiconductors and metal oxides have been successfully synthesized and studied. For the last few decades, ZnO has attracted much interest due to its versatile properties such as transparency in the visible range, direct band gap (3.37 eV), large exciton binding energy of 60 meV, absence of toxicity, etc. These qualities make it the best candidate for applications like transparent conducting electrodes in flat panel displays and window layers in solar cells [2-4]. It also exhibits many potential applications in areas such as laser diodes, solar cells, gas sensors, optoelectronic devices [5-7]. The ZnO nanoparticles can be synthesized using various techniques such as hydrothermal [8], sol-gel [9], wet chemical [10], precipitation [11], microemulsion [12], chemical vapor deposition [13], solid state reaction [14] and laser ablation [15]. The dielectric properties of an insulating medium can be modified by dispersing electrically conducting particles in the medium [16-19]. Thus the insulating host material can be modified into conducting or semi-conducting depending on the amount of filler particles dispersed in the medium [20- 22]. Zinc oxide is one of the most important basic components of rubber compounds. In rubber processing, it acts as an activator for the cross linking by sulphur or sulphur donors [23]. The rubber industry, utilized optical, physical and chemical properties of ZnO. It is the most effective activator to speed up the rate of cure. It can improve

*Corresponding author:deepuskariankal@gmail.com

the resistance to corona effects by its dielectric strength in high-voltage wire and cable insulation. The materials properties such as melting points, mechanical properties, and electrical properties change at nanoscale. The studies on the effect of frequency on the dielectric behaviour and a.c electrical conductivity give useful information about the conduction phenomenon in nanostructured materials. It was also noted that premelting of samples greatly depend upon the ac conductivity. And also the premelting of the mixtures at higher temperature led to a somewhat higher enhancement in ac conductivity because these temperatures are not high enough to allow for sintering or forming agglomerates [24]. The dielectric properties of particles are due to the contributions from electronic, ionic, dipolar and space charge polarizations. The determination of dielectric properties of the material is also important to assess the usability of the material in various electronic and optoelectronic applications.

In this work, the ZnO nanoparticles of different sizes were fabricated using the cost competitive and simple reverse micelle technique. In order to reduce the agglomeration among the smaller particles, the sodium dodecyl sulphide molecule which can bind to the surface of nanoparticles in the initial nucleation stage is used. Different samples were prepared by varying the calcination temperature. The ZnO nanoparticles are then characterised using UV-Visible spectrophotometer, IR spectrometer, Scanning electron microscope, transmission electron microscope and XRD. It was found that particle size increases with calcination temperature. So in order to find out the optimum temperature a TGA-DTA analysis of the sample was done. The prepared particles are then pressed into round disks of 1cm diameter and thickness 2mm. The disks were then coated with natural latex rubber using a microcontrolled dip coating unit. The dielectric properties of prepared nano ZnO-natural rubber disks are studied at room temperature.

2. Experimental

The ZnO nanoparticles were prepared by reverse micelle method. In a typical experiment, first solution was prepared by dissolving 8.636 g ZnSO_4 , 3.603 g CH_3COOH and 40 mg SDS as surfactant in 1 dm³ of water. The second solution was prepared by 3.6gNaOH pellets and 25ml 70% of ethanol. Then the first solution was slowly added to the second solution with continuous stirring. The obtained precipitate was filtered by using a Whatmann filter (grade-41) and air dried. The white solid product was washed with ethanol six times and with water ten times to remove impurities. Then, the dried precipitate was divided into four portions. The four portions were calcinated at 200 °C, 900°C, 750°C, and 550°C for one hour respectively. The samples were named as, A, B, C, D. The obtained powders were characterized using XRD, UV-Visible absorption Spectroscopy, FTIR, TEM and SEM. The TGA analysis of $\text{Zn}(\text{OH})_2$ was carried out using a TA instrument (SDT-2960) thermogravimetric analyser. The FTIR spectra were obtained using a SHIMADZU FTIR-8400S Japan in the range of 400 cm⁻¹ to 5000 cm⁻¹. The UV-Visible spectra of ZnO nano particle suspended in deionised water were recorded using an analytic Jena (Specord 50) spectrophotometer. X-ray diffractograms of ZnO nano powders were taken using a GE Inspection Technologies Seifert (PTS 3003) using a copper α radiation ($\lambda=1.54\text{\AA}$). Scanning electron micrographs of ZnO nano particles were obtained by (Philips XL 30) SEM. Transmission electron micrographs were taken in a JEOL Crop. (JEM – 3010) TEM microscope at an accelerating voltage of 100KV.

The samples were then made into disks of 1cm diameter and 2mm thickness. The disks were coated with a 0.5mm layer of natural rubber using dip coating technique.

2.1 Dielectrical studies

These studies were carried out using a Hioki LCR Impedence analyzer (model 3532-50) in the frequency range of 100 KHz to 5MHz, at room temperature. The samples were inserted between two copper plates of the same diameter to form a capacitor in a home-made dielectric cell whose fabrication details are reported elsewhere [25]. Using the impedance analyzer, the capacitance and loss tangent were measured at different intervals using an automated measurement set-up.

3. Results and discussion

3.1 Thermogravimetric analysis

A Thermogram of $\text{Zn}(\text{OH})_2$ heated from room temperature to 800°C in nitrogen atmosphere is shown in fig. 1. It is clearly seen in the curves that the mass loss begins just below 200°C and the rate of mass loss increases with increasing in temperature up to 500°C , after which the mass becomes constant. The constant mass indicates that all the $\text{Zn}(\text{OH})_2$ has been converted into ZnO .

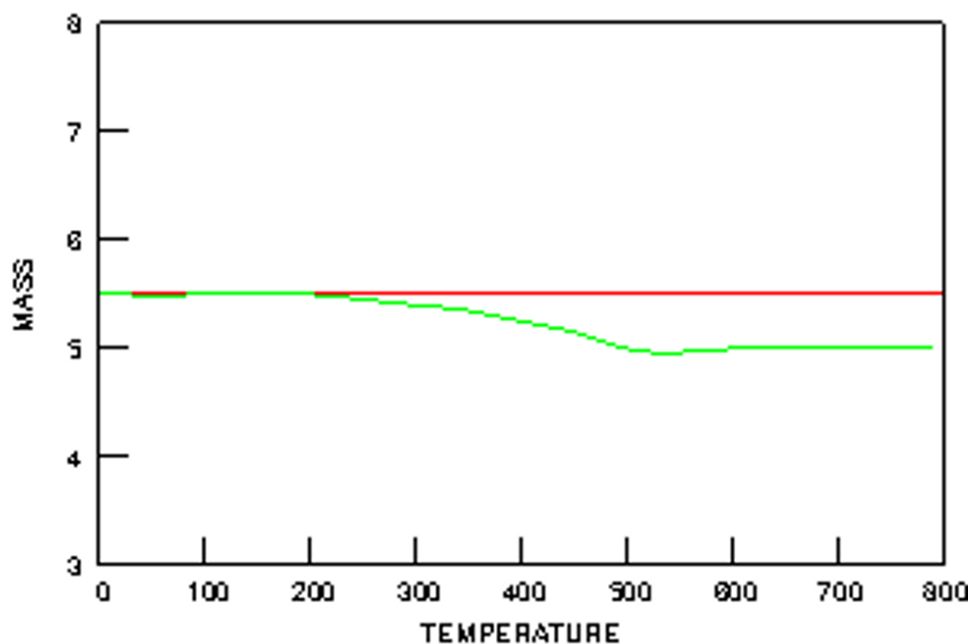


Fig. 1. Thermogram of $\text{Zn}(\text{OH})_2$

3.2 Spectroscopic analysis

3.2.1 FTIR spectroscopy

The fig. 2a, 2b, 2c and 2d show the FTIR spectra of ZnO powders heat treated at 200°C , 550°C , 750°C , and 900°C . For the powders heat treated at 900°C only the band due to the Zn-O bond at 500 cm^{-1} is seen. IR spectra of powders heat treated at 550°C show bands near 1517 cm^{-1} ($\text{C}=\text{O}$ stretching mode), 2339 cm^{-1} (due to the adsorption of CO_2 from atmosphere on the metallic cation and a band at 500 cm^{-1} (Zn-O). The IR spectra of powder heat treated at 200°C shows many strong bands. This shows that $\text{Zn}(\text{OH})_2$ does not change completely into ZnO . The intensity and position of the band near 500 cm^{-1} is similar in all cases, indicating that temperature will not affect the Zn-O bond.

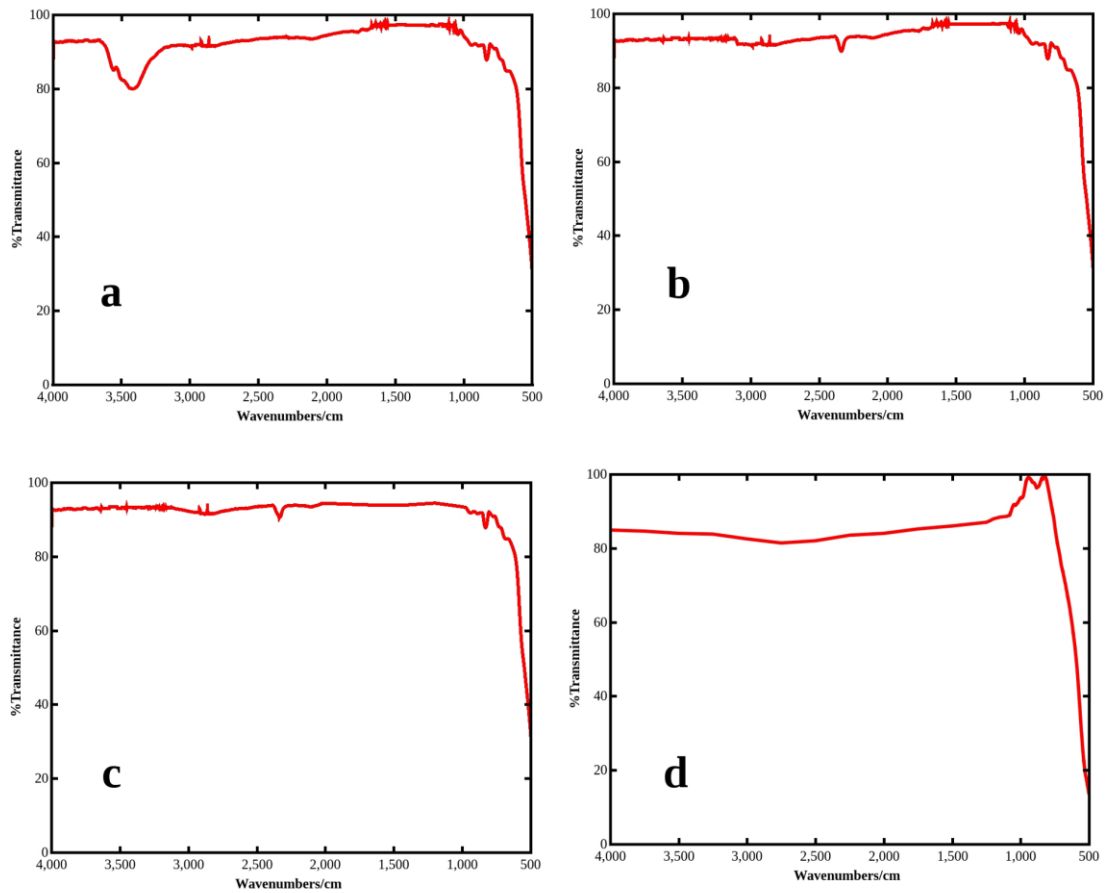


Fig. 2. FTIR spectra of ZnO powders heat treated at (a) 200°C, (b) 550°C (c) 750°C and (d) 900°C

3.2.2 UV-VISIBLE spectroscopy

Fig. 3 shows UV-VISIBLE absorption spectras of the B, C and D samples of nano ZnO powder. The prepared nano powders were first dispersed in water and then the UV-VIS optical absorption characteristics were measured. The presence of ZnO nanoparticles is clearly evident in fig.3. The excitonic absorption peak for sample heat treated at 550°C is observed at 361.34 nm, which lies much below the bandgap wavelength of 388 nm ($E_g = 3.3$ eV) of micro ZnO. The Figure shows absorption peak at 370 nm for sample heat treated at 750°C and the sample heat treated at 900°C shows peak at 378 nm. Also it is observed that absorption of ZnO is very sharp, which indicates the mono dispersed nature of the nanoparticle distribution. The mono dispersed nature of particle distribution has also been confirmed by SEM and TEM measurement.

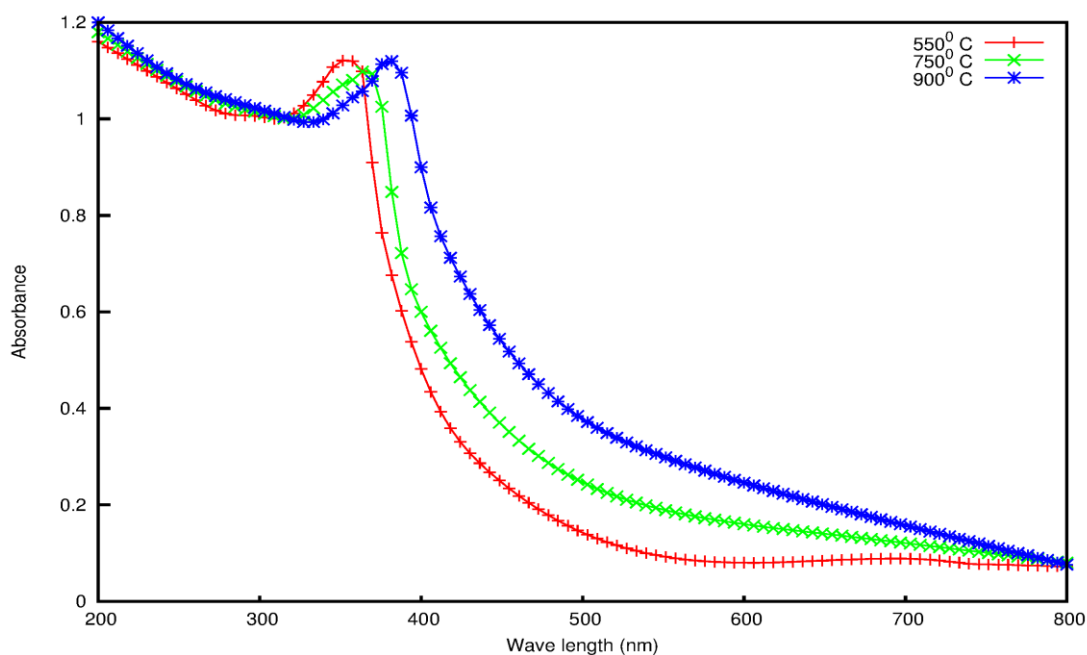


Fig. 3. UV-VISIBLE absorption spectra of nano ZnO powder at various temperatures

Only the largest particles contribute to the absorbance, at the absorption edge. But in case of the smaller wavelength range, particles with smaller sizes contribute more. At the region of absorbance maximum, all particles contribute to the absorbance. Thus the average particle size present in a nano colloid can be obtained from the inflection point in the uv spectrum. Equation (1) based on the effective mass model, gives the relation between the particle size (r , radius) and the peak absorbance wavelength (λ_p) for mono dispersed ZnO nano colloid. ZnO nano particles prepared at 550°C show peak absorbance at ~361 nm which corresponds to average particle size of 52.34 nm.

$$r(\text{nm}) = \frac{-0.3049 + \sqrt{-26.23012 + \frac{10240.72}{\lambda_p(\text{nm})}}}{-6.3829 + \frac{2483.2}{\lambda_p(\text{nm})}} \quad (1)$$

3.3 XRD studies

Fig. 4 shows XRD patterns of nano ZnO crystals. The broadening in the XRD peaks reveals the nanocrystalline nature of the particles. The broadening of the peaks decreases with increasing calcinations temperature showing that size increases with increase in temperature. X ray diffraction patterns are obtained when incident X-rays are scattered by the parallel planes in the particles. As the powder size decreases, the planes in them rearrange so that the number of parallel planes decreases. Because of this the peaks broadens. The particle size was calculated using the Scherer equation, $D = 0.9\lambda / \beta \cos\theta$ where D is the particle size, λ is the wavelength, β is the full width at half maximum and θ is the diffraction angle. X ray diffractograms of nano ZnO calcinated at various temperatures shows a maximum intense peak is at the 2θ value 36.2° and d (interplanar distance) value 2.48056 indicates hexagonal crystal structure of ZnO and this peak broadens with decrease in particle size. As the calcination temperature increased from 200°C to 900°C the size of the particles increased from 22nm to 66nm. As mentioned earlier, the formation of ZnO is incomplete at 200°C.

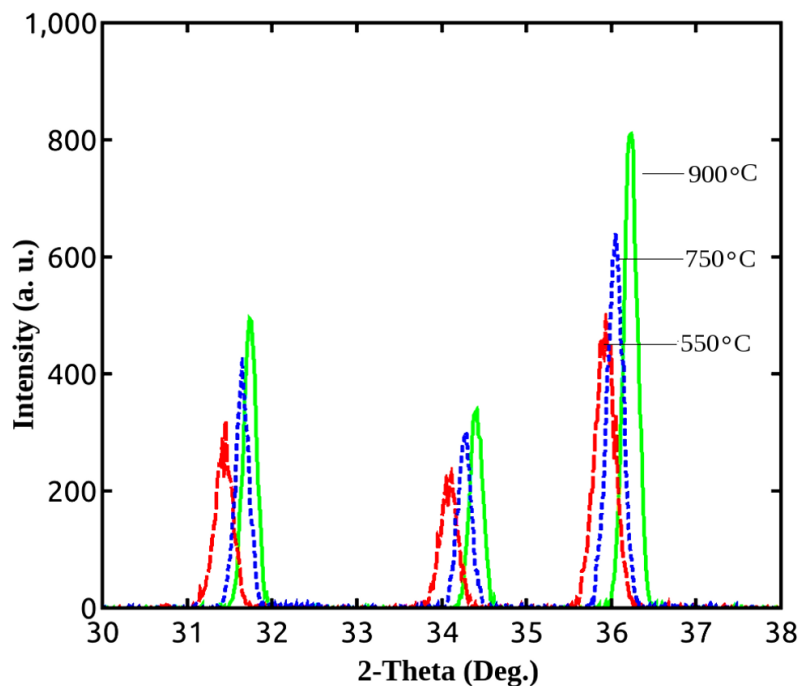


Fig. 4. X ray diffraction patterns of ZnO heat treated at various temperatures

3.3.1 Effect of calcination temperature on metal oxide nanoparticles

The fig. 5 shows variation of average particle size of powders with different calcination temperatures. The particle size increases with increase in calcination temperature. The XRD studies and SEM micrographs clearly show this. SEM shows that the shape changes from spherical to hexagonal. The size of the crystal is proportional to its surface energy, hence small crystals get converted into large crystals automatically. The process happens immediately, especially at high temperature. The process becomes complete with prolonged calcination time. The crystal size increases with the calcination temperatures [26]. And it leads to the acquisition of large size nanoparticles.

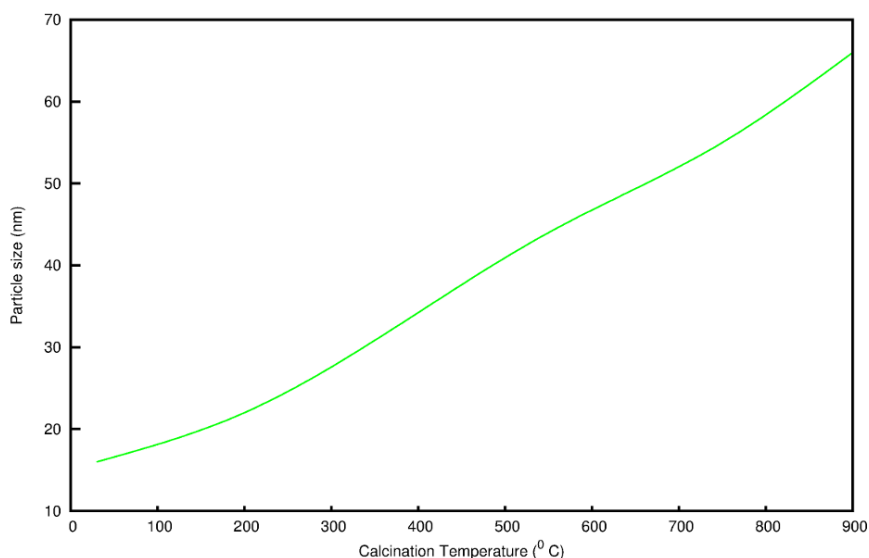


Fig. 5. variation of particle size with calcination temperature (obtained from XRD data)

3.4 Microscopic analysis

3.4.1 Scanning electron microscopy

The scanning electron micrographs of nanocrystalline ZnO powders are shown in figure 6. As seen in the figure, the powder calcined at 900°C (fig. 6a) has hexagonal structure and the particles have size in the range of a few hundred nanometres. As we decrease the temperature, it can be seen that the size decreases and the shape changes from hexagonal to almost spherical. At 550°C (fig. 6b) the size is around 40 nm and at 200°C (fig. 6c) the size is around 20 nm. The size obtained from scanning electron micrographs is in agreement with size obtained from XRD.

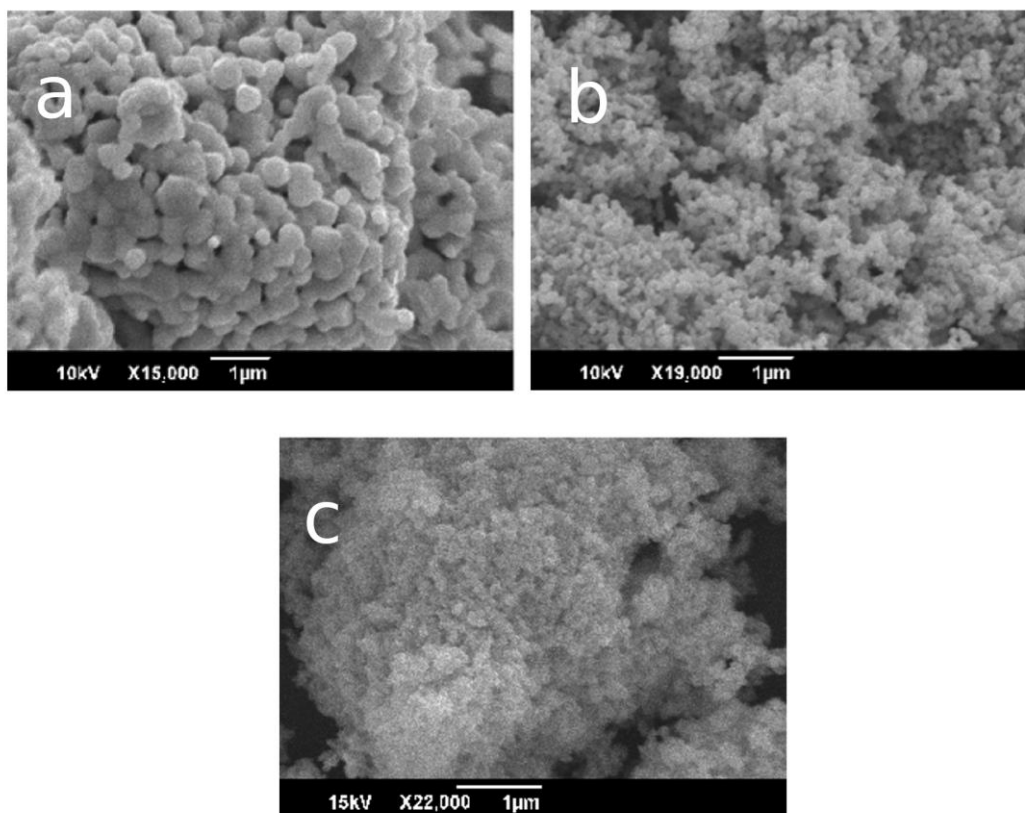


Fig. 6. SEM micrographs of nano ZnO (a) at 900°C (b) at 550°C and (c) at 200°C

3.4.2 Transmission Electron microscopy

The formation of the metal oxide nanoparticles can be easily proved by Transmission electron microscopy. Fig. 7 shows TEM images recorded from drop coated films of the ZnO nano particles prepared by calcination at 550°C. The particles are mono disperse in nature with an average size of 40-60nm. The nanoparticles are predominantly spherical in shape. Fig. 7a and 7b both include a scale for comparison.

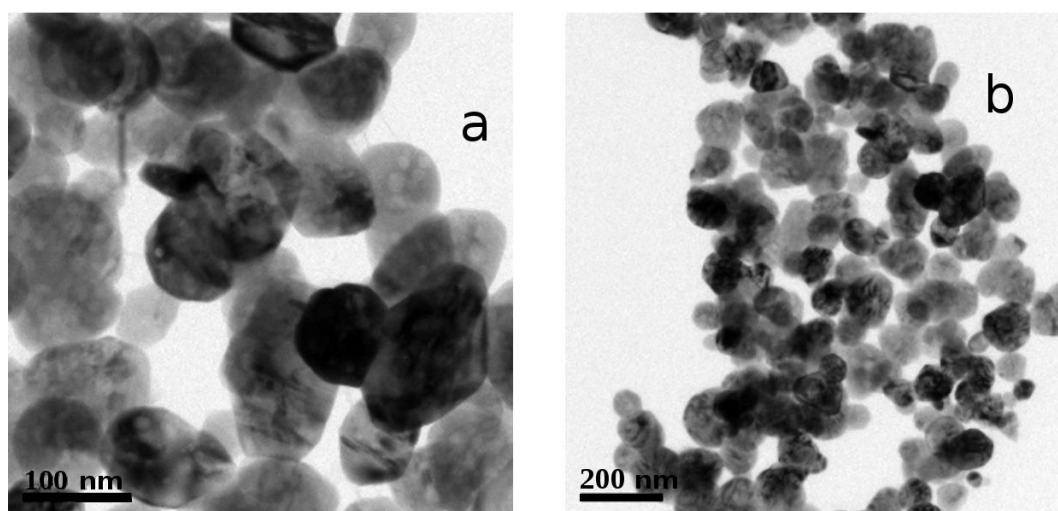


Fig. 7. TEM Micrographs of ZnO nanoparticles.

3.5 Dielectric Studies

The electrical properties of a dielectric substance are usually described in terms of dielectric constant and dielectric loss. The variation of dielectric constant as function of frequency at room temperature of samples A, B, C and D is shown in the figure 8a. The dielectric constant or relative permittivity is determined using the equation $\epsilon_r = C.d / \epsilon_0 A$, where C is the capacitance of the sample, d and A are the thickness and area of the sample pellet. The figure 8a shows the variation of dielectric constant with frequency at room temperature. It is clear from the results that the dielectric constant remains fairly constant at higher frequencies. Here dielectric constant decreases with the increasing frequency for all the samples. At lower frequency (100 KHz), this effect is more prominent. Increase in dielectric constant in nano ZnO–rubber disks is nearly inversely with the particle size of the ZnO particles. In this case sample D possesses more dielectric constant compared to other samples, but the sample A dielectric constant is low because of the incomplete formation of ZnO. The space charge effect will be a prominent factor, in determining the dielectric properties in materials with small particle sizes [27, 28]. In addition, ion jump polarization may also be greater in nanocrystalline materials since there will be a number of positions at the grain boundaries for the ions to occupy. The high values of the dielectric constant in the present study may be attributed to the increased ion jump orientation effect and the increased space charge effect exhibited by nanoparticles. The variations of dielectric loss factor ($\tan\delta$) of samples A, B, C, and D with different frequency are shown in figure 8b. It can be seen that the dielectric loss shows the behaviour similar to that of the dielectric constant. In dielectric materials, dielectric losses usually occur due to absorption current. In nanophase materials, inhomogeneities like defects and space charge formation in the interphase layers produce an absorption current resulting in a dielectric loss. Hence It is possible to obtain a desired dielectric constant in conjunction with small dielectric loss. The samples are thus potential candidates for making capacitors [26]. With the addition of a rubber coating to assure mechanical integrity, the disk becomes a practical candidate for capacitor manufacture. The a.c conductivity of the samples was calculated using the equation. $\sigma_{ac} = 2\pi f \epsilon_0 \epsilon_r \tan\delta$ [22] and shown in the figure 8c, where f is the frequency, ϵ_0 is the permittivity of free space, ϵ_r is the relative permittivity of the sample and $\tan\delta$ is the dielectric loss factor. The ac conductivity increases with increase in frequency. The a.c. conductivities strongly depend on the particle size, the concentration and heat treatment of the sample and the premelting of the electrolytes [24]. It can be seen that σ_{ac} increases with frequency for samples A, B, C and D in a sequential order. Here a.c conductivity of sample D is few orders

higher than the other samples. The increase of a.c. conductivity with the frequency indicates that the mobility of charge carriers is responsible for hopping [29]. The electrons which are involved in hopping are responsible for the electronic polarization in nano ZnO rubber disks.

3.5.1 Q – Factor

The Q-factor of samples is measured in the frequency range of 100 KHz to 5 MHz. The Fig. 8d explains the plot of Q-factor versus frequency of nano ZnO-rubber disks, i.e. Sample A, B, C, and D. It can be seen that Q-factor increases with frequency for all the samples. For the sample A Q-factor is much low compared to other samples.

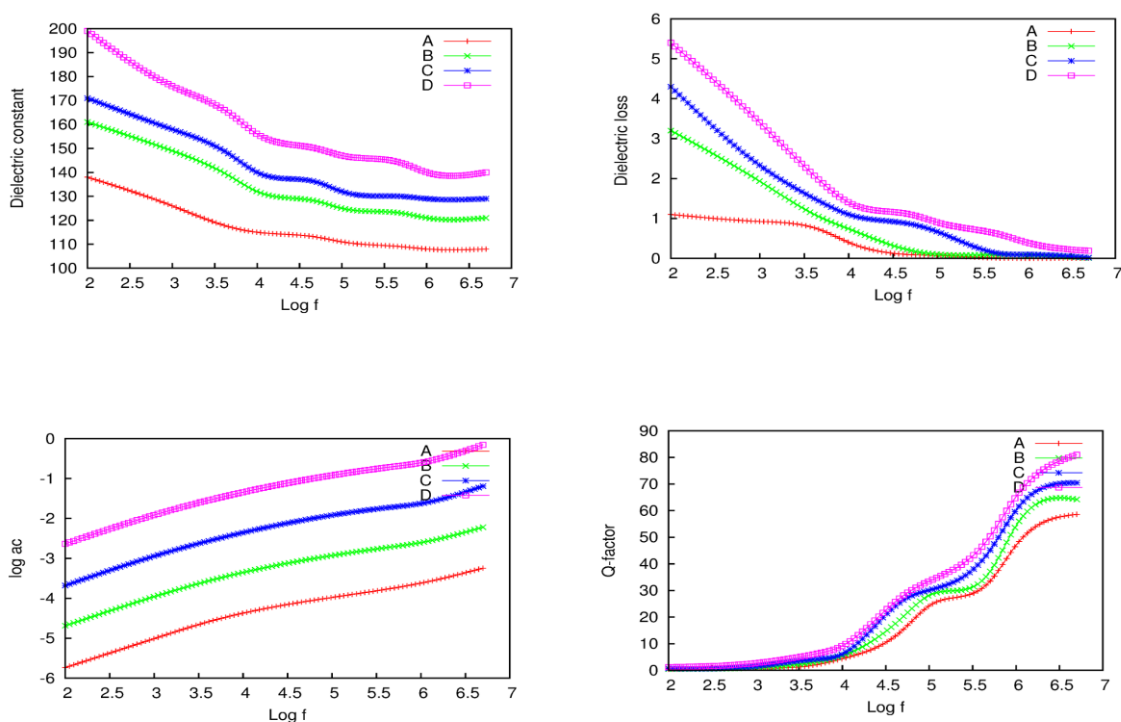


Fig. 8. (a) Variation of dielectric constant with Log f, (b) Variation of dielectric loss with Log f (c) Variation of ac conductivity with Log f (d) Variation of Q- Factor with Log f

4. Conclusion

In the present study ZnO nanopowders were synthesised successfully with sodium dodecyl sulphide as the stabilising agent. The monodisperse nano size of the prepared particles was confirmed by different characterising techniques. In this investigation the direct relationship of particle size with calcination temperature was well established. The dielectric studies of the rubber coated disks prepared from the nano ZnO particles of different size were carried out. It was found that the dielectric properties vary with particle size. By changing the particle size we can tune the dielectric parameters to the desired value. This finding permits the fabrication of electronic and optoelectronic devices with improved characteristics. The high value of dielectric constant for nano ZnO-natural rubber disks enhances its property towards nanoscale charge storage devices which is an essential prerequisite for biomedical applications.

Acknowledgment

The authors are grateful to Prof. Mike Raleigh, retired physicist from Pennsylvania State University USA, 16802, for the valuable help he rendered regarding the manuscript.

Reference

- [1] G. Shan, X. Kong, X. Wang, Y. Liu. *Surf. Sci.* **582**, 61 (2005).
- [2] Z.L. Wang. *J. Physics:Condensed Matter.* **16**, 829 (2004).
- [3] Z. Fan , J.G. Lu. *J. Nanoscience and Nanotechnology.* **5**(10), 1561 (2005).
- [4] S. Baruah, J. Dutta. *Sci. Technol. Adv. Mater.* **10**(1), (2009).
- [5] D. S. Mao, X. Wang, W. Li, X. H. Liu, Q. Li, J. F. Xu. *J. Vac. Sci. Technol. B.* **20**, 278 (2002).
- [6] Y. W. Zhu, H. Z. Zhang, X. C. Sun, S. Q. Feng, J. Xu, Q. Zhao, B. Xiang, R. M. Wang and D. P. Yu. *Appl. Phys. Lett.* **83**, 144 (2003).
- [7] W.Z. Wang, B.Q. Zeng, J. Yang, B. Poudel, J.Y. Huang, M.J. Naughton and Z.F. Ren. *Adv.Mater.* **18**, 3275 (2006).
- [8] A. Rabenau, *Angew. Chem. Int. Ed. Engl.* **24**, 1026 (1985).
- [9] J. Huang, N. Matsunaga, K. Shimanoe, N. Yamazoe, T. Kunitake. *Chem. Mater.* **17**, 3513 (2005).
- [10] A. Yadav, V. Prasad, A. Kathe, S. Raj, D. Yadav, C. Sundaramoorthy, N. Vigneshwaran. *Bull. Mater. Sci.* **29**, 641 (2006).
- [11] N. Izu, N. Murayama, W. Shin, T. Itoh, I. Matsubara. *Mater. Lett.* **62**(2), 313 (2008).
- [12] Y. Liu, C. Zheng, W. Wang, C. Yin, G. Wang, *Adv. Mater.*, **13**, 1883 (2001).
- [13] Y. K. Liu, C. L. Zheng, W. Z. Wang, Y. J. Zhan, G. G. Wang, *J. Cryst. Growth.* **233**, 8 (2001).
- [14] C. K. Xu, G. D. Xu, Y. K. Liu, X. L. Zhao, G. H. Wang. *Scripta Mater.* **46**, 789 (2002).
- [15] D. F. Zhang, L. D. Sun, J. L. Yin, C. H. Yan. *Adv. Mater.* **15**, 1022 (2003) .
- [16] T. Tanaka, G.C. Montanari, R. Mulhaupt. *IEEE Trans. Dielect. Electr. Insul. II.* **11**(5), 763 (2004).
- [17] G. M. Tsangaris, G. C. Psarras, A. J. Kontopoulos. *J. Non-Cryst. Solids.* **131**, 1164 (1991).
- [18] G. C. Psarras, E. Manolakaki, G. M. Tsangaris. *Composites Part A.* **33**, 375 (2002).
- [19] G. C. Psarras, *Composites Part A.* **37**(10), 1545 (2006).
- [20] P. S. Neelakanta. *Handbook of Electromagnetic Materials*, CRC Press, (1995).
- [21] B. Zhang, Y. Feng, J. Xiong, Y. Yang, H. Lu. *IEEE Trans. Magn.* **42**(7), 1778 (2006).
- [22] S. Sindhu, M.R. Anantharaman, B.P. Thampi, K. A. Malini, P. Kurian. *Bull. Mater.Sci.* **25** (7), 599 (2002).
- [23] F. W. H. Kruger , W. J. Mc Gill. *J. Appl.Polym Sci.* **42**, 2643 (1991).
- [24] K. Shah1, J. B. Wagner. *J. Solid State Chemistry.* **42**, 107 (1982).
- [25] E. Muhammad Abdul Jamal, P. A. Joy, P. Kurian, M. R. Anantharaman, *Materials Science and Engineering B*,**156**, 24 (2009).
- [26] L. E. Shi, X. J Fang, Z. L Zhang, T. Zhou, D. Jiang, H. Wu, Z. X. Tang. *Int. J. Food Sci. Tech.*, **47**, 1866 (2012).
- [27] Y. P. Xu, W. Y. Wang, D. F. Zhang, X. L. Chen. *J. Mater. Sci.* **36**, 4401 (2001).
- [28] W. Y. Wang, Y. P. Xu, D. F. Zhang, X. L. Chen. *Mater. Res. Bull.* **36**, 2155 (2001).
- [29] T. Moumit Ghosh, C. N .R. Rao, *Chem. Phys. Lett.* **393**, 493 (2004).